© 2016 IJSRSET | Volume 2 | Issue 2 | Print ISSN : 2395-1990 | Online ISSN : 2394-4099
Themed Section: Engineering and Technology

Annealing Effect on Microstructure, Hardness and Electrochemical Corrosion Behavior of Copper- Manganese Alloy

Abu Bakr El-Bediwi[1], S. Bader[1], Zuhor Farag [1, 2]

[1]Metal Physics Lab., Physics Department, Faculty of Science, Mansoura University, Egypt
[1, 2]Faculty of Education Janzor, University of Tripoli, Libya

ABSTRACT

The $Cu_{98}Ge_2$ alloy was annealed at 500 °C, 600 °C and 700 °C for 2 hours and characterized by x-ray diffractmeter, scanning electron microscope, digital Vickers micro-hardness tester and Gamry Potentiostat/Galvanostat with a Gamry framework system based on ESA 300. X-ray and scanning electron microscope analysis show a significant change on microstructural of $Cu_{98}Mn_2$ alloy after annealing at different temperature for 2 hours. Lattice microstrain of $Cu_{98}Mn_2$ alloy varied after annealed at different temperature for two hours. Vickers hardness and corrosion rate values of $Cu_{98}Mn_2$ alloy increased after annealing at different temperature for 2 hours. Corrosion current of $Cu_{98}Mn_2$ alloy decreased after annealing at 500 °C and 600 °C but it increased at 700 °C for 2 hours. The best annealing temperature for $Cu_{98}Mn_2$ alloy is 500 °C for 2 hours.

Keywords: Corrosion Behavior, Vickers Hardness, Internal Friction, Elastic Moduli, Electrical Resistivity, Lead-Calcium Alloys

I. INTRODUCTION

Many types of copper and copper alloy are used and their compositions roughly grouped into copper, high copper alloy, brasses, bronzes, copper nickels, copper-nickel-zinc and leaded copper. High copper alloys contain small amounts of alloying elements such as nickels or manganese or aluminum or chromium or zirconium or tin or silver or iron. Alloying elements modify one or more of the basic properties of copper, such as strength, creep resistance, machinability or weldability. The shape-memory effect is strongly influenced by many heat-treatment parameters, such as betatizing temperature, betatizing duration and rate of quenching [1]. Annealing for 2 and 4 hours at 120, 140 and 160 °C caused variations in the elastic modulus, internal friction and stiffness of tin- antimony alloys [2]. Ultimate tensile strength of Sn- 5%Sb, Sn- 5%Sb- 1.5%Bi and Sn- 5%Sb- 1.5%Cu alloys increased with increasing strain rate and decreased with increasing temperature [3]. The ductility decreased with increasing strain rate, but it exhibited some fluctuation with temperature. Adding SiC, Al_2O_3, TiB_2 and TiC as a hard inclusion significantly improve the mechanical properties of copper matrix materials with keeping high electrical and thermal conductivity [4- 6]. Low price Al_2O_3 particles have mostly selected as the reinforcement phase for copper matrix alloys [7, 8]. Also the uniform distribution of Al_2O_3 particles can be accomplished by the process of internal oxidation [9, 10] or by mechanical alloying [11, 12]. The aim of this work was to study the effect of annealing at different temperature for 2 hours on microstructure, hardness and electrochemical corrosion behavior of copper-manganese alloys.

II. METHODS AND MATERIAL

Commercial bare of $Cu_{98}Mn_2$ (98 wt. % Cu and 2 wt. % Mn) alloy was provided via the European Copper Institute, Brussels. The bare samples were cut to suitable dimensions for different measurements. These alloy bars annealed at temperatures 500 °C, 600 °C and 700 °C for two hours in electric furnace. Microstructural of used alloys was studied using a Shimadzu x–ray diffractometer (Dx–30, Japan) and scanning electron microscope (JEOL JSM-6510LV, Japan). Vickers hardness value of used alloys was measured using A digital Vickers micro-hardness tester, (Model-FM-7- Japan). The polarization studies were performed using Gamry Potentiostat/Galvanostat with a Gamry framework system based on ESA 300. Gamry applications include software DC105 for corrosion measurements, and Echem Analyst version 5.5 software packages for data fitting. The working electrode was immersed in the acid solution and the constant steady-state (open circuit) potential was recorded when it became virtually constant. The polarization studies were carried out over a potential of +250 to -250 mV with respect to the open circuit potential at a scan rate of 5 mV s^{-1}. The linear Tafel segments of the anodic and cathodic curves were extrapolated to obtain corrosion potential (E_{corr}) and corrosion current density (j_{corr}).

III. RESULTS AND DISCUSSION

A. Microstructure

X-ray diffraction patterns of $Cu_{98}Mn_2$ alloy before and after at 500 °C, 600 °C and 700 °C for 2 hours are shown in Figure 1 (a, b, c and d). Figure 1b shows $Cu_{98}Mn_2$ alloy after annealed at 500 °C for 2 hours, there is a change in intensity peak (counts decreased from 2000 to 1000), began base line (amorphous area or random distribution of atoms) and position (orientation of atoms). After annealed $Cu_{98}Mn_2$ alloy at 600 °C for 2 hours there is also change in intensity peak (counts decreased from 2000 to 1200), amorphous area become homogenous and began from 2θ= 0 to 38° as shown in Figure 1c. Figure 1d shows $Cu_{98}Mn_2$ alloy after annealed at 700 °C for 2 hours, there is a change in intensity peak (counts decreased from 2000 to 700), amorphous area become homogenous with increasing hump compared to its annealed at 600 °C and began from 2θ= 0 to 36.5°. From x-ray analysis listed in Table 1 b after annealed $Cu_{98}Mn_2$ alloy at 500 °C, some peaks (phases) disappeared like at 2θ=34.846°, 40.6248° and 58.7363° and the intensity of Cu phase increased after annealed at 500 °C for 2 hours. Table 1c shows, when the $Cu_{98}Mn_2$ alloy annealed at 600 °C some peaks disappeared like at 2θ=34.846°, 40.6248°, 58.7363°, 61.2382° and 89.7605° and the intensity of Cu phase changed. But Table 1d when the alloy annealed at 700 °C some peaks disappeared like at 2θ=34.846°, 40.6248°, 58.7363° and 89.7605° and the intensity of Cu phase changed. From these results it's clear that, significant changed in structure (formed phases such as intensity, broadness, area and position) of $Cu_{98}Mn_2$ alloy after annealing at different temperature for two hours. From the relation between full width half maximum (β) and 4tanθ [13, 14] as shown in Figure 1e, the induced internal lattice microstrain of $Cu_{98}Mn_2$ alloy before and after at 500 °C, 600 °C and 700 °C for 2 hours alloys were calculated and then listed Table 1e. Lattice microstrain of $Cu_{98}Mn_2$ alloy varied after annealed at different temperature for two hours.

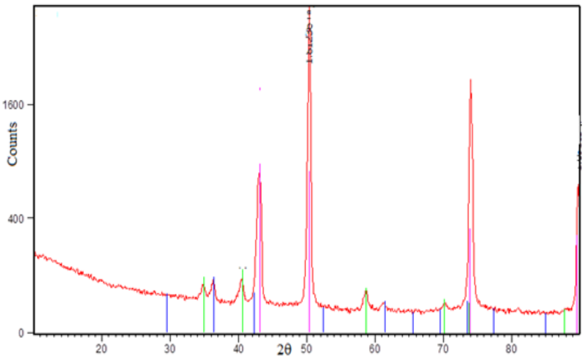

Figure 1a : x-ray diffraction patterns of $Cu_{98}Mn_2$ alloy

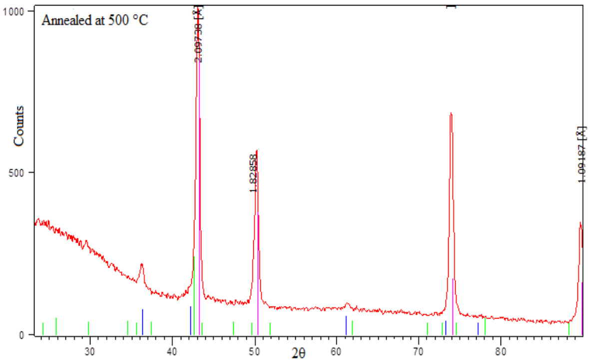

Figure 1b : x-ray diffraction patterns of $Cu_{98}Mn_2$ alloy after annealed at 500 °C for 2 hours

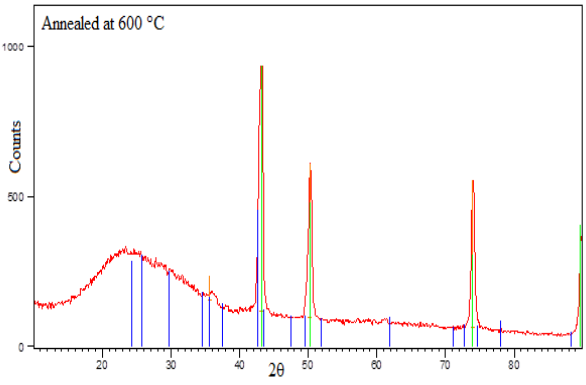

Figure 1c : x-ray diffraction patterns of $Cu_{98}Mn_2$ alloy after annealed at 600 °C for 2 hours

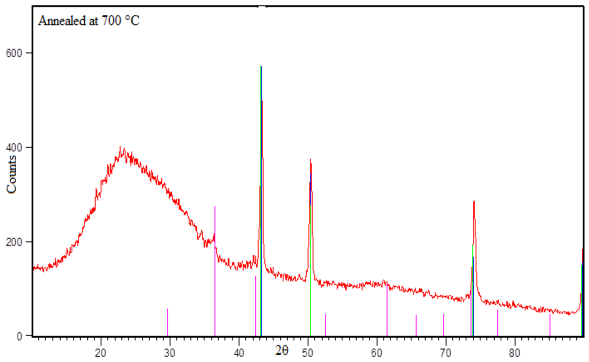

Figure 1d. x-ray diffraction patterns of $Cu_{98}Mn_2$ alloy after annealed at 700 °C for 2 hours

Table 1a: x-ray analysis of $Cu_{98}Mn_2$ alloy

2θ	d Å	Int. %	FHWM	Area	Phase	hkl
34.846	2.575	1.07	0.6298	21.53	CuMn	
36.3915	2.469	1.62	0.4723	24.36	Cu_2O	111
40.6248	2.221	1.53	0.4723	23.05	CuMn	
43.1918	2.09	22.48	0.2362	169.49	Cu	111
50.349	1.812	100	0.3936	1256.7	Cu	200
58.7363	1.572	1.2	0.551	21.08	CuMn	
61.2382	1.514	0.33	0.9446	10.05	Cu_2O	220
73.976	1.281	58.47	0.2952	551.07	Cu	200
89.7605	1.09	20.42	0.264	232.64	Cu	311

Table 1b: x-ray analysis of $Cu_{98}Mn_2$ alloy annealed at 500 °C for 2 hours

2θ	d Å	Int. %	FHWM	Area	Phase	hkl
36.3719	2.47	18.54	0.6727	160.8	Cu_2O	111
43.1319	2.097	100	0.001	1.29	Cu	111
49.8719	1.829	28.12	0.001	0.36	Cu	200
61.2119	1.514	5.12	0.09	5.94	Cu_2O	220
73.9064	1.282	66.68	0.9557	821.6	Cu	200
89.8319	1.092	30.39	0.001	0.39	Cu	311

Table 1c: x-ray analysis of $Cu_{98}Mn_2$ alloy annealed at 600 °C for 2 hours

2θ	d Å	Int. %	FHWM	Area	Phase	hkl
35.57	2.524	8.21	0.001	0.05	Cu_2O	111
43.2285	2.093	100	0.3542	350.6	Cu	111
50.2697	1.815	51.49	0.2165	110.32	Cu	200
74.006	1.28	48.99	0.384	251.65	Cu	200

Table 1d: x-ray analysis of $Cu_{98}Mn_2$ alloy annealed at 700 °C for 2 hours

2θ	d Å	Int. %	FHWM	Area	Phase	hkl
36.35	2.472	38.75	0.001	0.24	Cu_2O	111
43.2812	2.09	100	0.4187	257.33	Cu	111
50.4072	1.81	72.2	0.3822	169.64	Cu	200
61.11	1.52	11.55	0.09	6.39	Cu_2O	220
74.11	1.28	54.98	0.001	0.34	Cu	200

Table 1e: - lattice microstrain of $Cu_{98}Mn_2$ alloy before after annealed at different temperature for 2 hours

$Cu_{98}Mn_2$ alloy	$\varepsilon \times 10^{-4}$
Before	11
500 °C	2
600 °C	28
700 °C	21

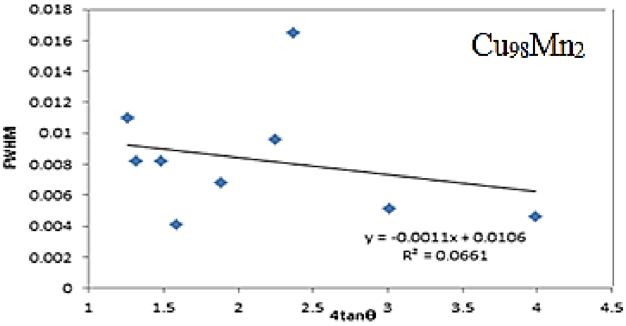

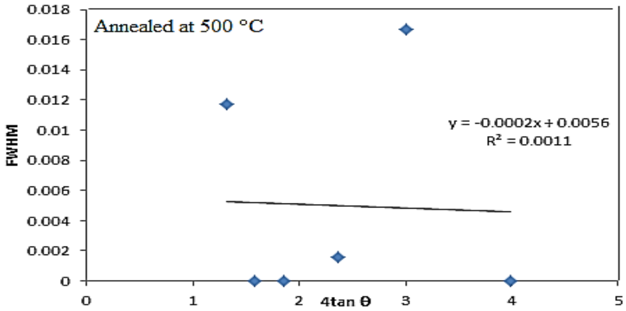

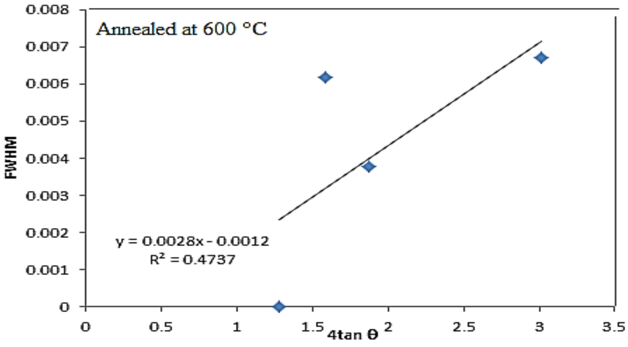

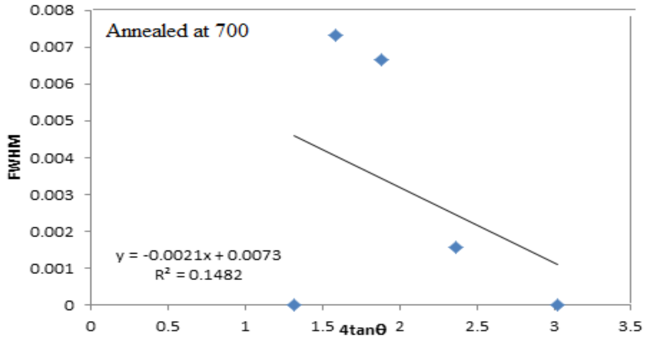

Figure 1e. FWHM versus 4tanθ for used alloys

Scanning electron micrographs analysis

Scanning electron micrographs (SEM) of $Cu_{98}Mn_2$ alloy before and after annealed at 500 °C, 600 °C and 700 °C for 2 hours are shown in Figure 2 (a, b, c and d). Figure 2b shows SEM of $Cu_{98}Mn_2$ alloy annealed at 500 °C for two hours which consists of lamellar structure (different size from ~1 µm to 4 µm, length and orientation), group of grains (different size, length of grain from ~ 35 µm and height ~ 20 µm) spread between two large lamellar structures and other grains spread (white and black color) in matrix alloy. SEM of $Cu_{98}Mn_2$ alloy annealed at 600 °C for two hours consists of lamellar structure with homogenous matrix alloy as seen in Figure 2c and other small grains spread (white and black color) in matrix alloy. Also SEM of $Cu_{98}Mn_2$ alloy annealed at 700 °C for two hours consists of intersection lamellar structure (different size, length and orientation) as shown in Figure 2d and large dendrite structure contains different grain size with other small grains spread in matrix alloy.

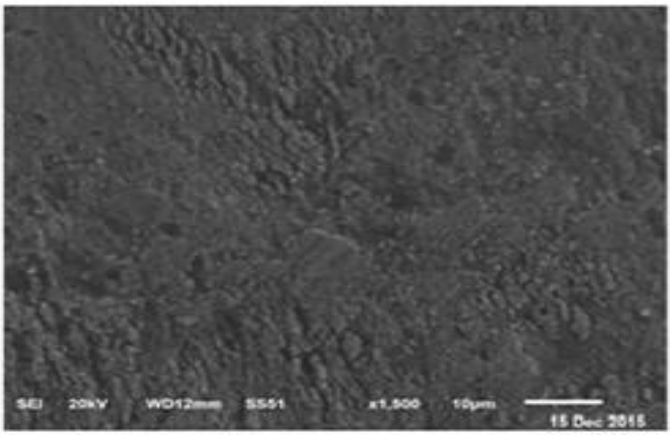

Figure 2a. SEM of $Cu_{98}Mn_2$ before annealing

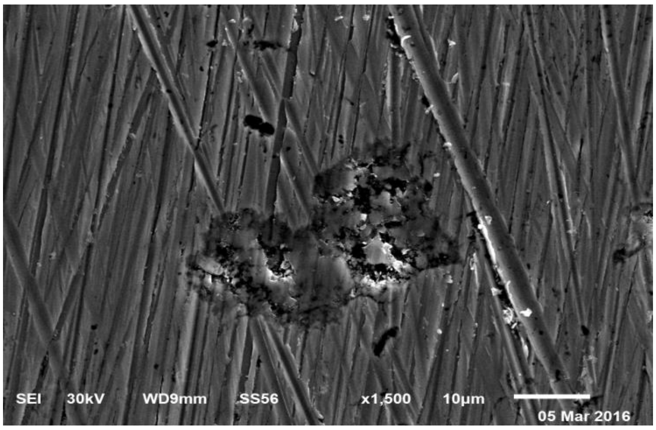

Figure 2b. SEM of $Cu_{98}Mn_2$ annealed at 500 °C for two hours

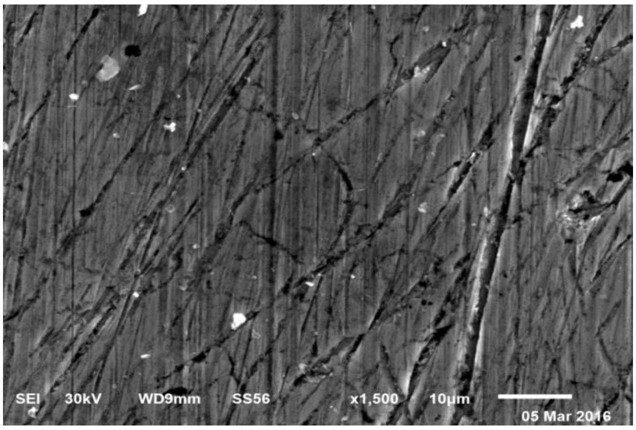

Figure 2c. SEM of $Cu_{98}Mn_2$ annealed at 600 °C for two hours

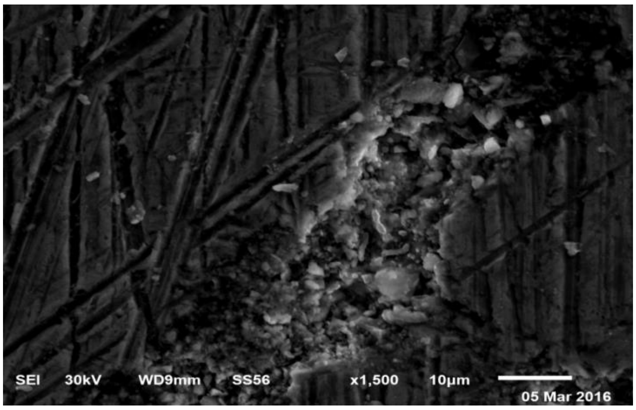

Figure 2d.SEM of $Cu_{98}Mn_2$ annealed at 700 °C for two hours

B. Vickers hardness and shear stress

In materials science, the definitions of hardness are the scratch hardness which is resistance to fracture (or plastic deformation) due to friction from a sharp object or the indentation hardness which is resistance to plastic deformation due to impact from a sharp object or the rebound hardness which is height of the bounce of an object dropped on the material, related to elasticity. Vickers hardness and calculated maximum shear stress values of $Cu_{98}Mn_2$ alloy before and after annealed at 500 or 600 or 700 °C for two hours are listed in Table 2. Vickers hardness of $Cu_{98}Mn_2$ alloy increased after annealed at 500 or 600 or 700 °C for two hours. That is meant, the strength of $Cu_{98}Mn_2$ alloy increased after annealing. That is because annealing caused a change in alloy microstructure such as formed strengthen points in matrix alloy (grains spread in matrix and forming different lines as lamellar structure) due to diffusion mechanism.

Table 2. Vickers hardness and maximum shear stress of $Cu_{98}Mn_2$ alloy before and after annealed for 2 hours

$Cu_{98}Mn_2$ alloy	H_v kg/mm^2	μ_m kg/mm^2
before	44.475±3.17	14.68
500 °C	62.6±6.35	20.66
600 °C	76.76±5.58	25.33
700 °C	91.84±9.18	30.31

C. Electrochemical Corrosion Behavior

Figure 3 shows electrochemical polarization curves of $Cu_{98}Mn_2$ alloy before and after annealed at 500 or 600 or 700 °C for two hours in 0.25 M HCl. From these results, the corrosion potential of used alloys exhibited a negative potential. Also the cathodic and the anodic polarization curves exhibited similar corrosion trends. The corrosion current (I_{Corr}), corrosion potential (E_{Corr}) and corrosion rate (C. R) of used alloys in 0.25 M HCl are listed in Table 3. Very little variation occurred in corrosion rate of $Cu_{98}Mn_2$ alloy after annealing at 500 or 600 °C for two hours. Significant increased occurred in corrosion current and corrosion rate of $Cu_{98}Mn_2$ alloy after annealing at 700 °C for two hours. The $Cu_{98}Mn_2$ alloy annealed at 500 °C has low values of corrosion current and corrosion rate.

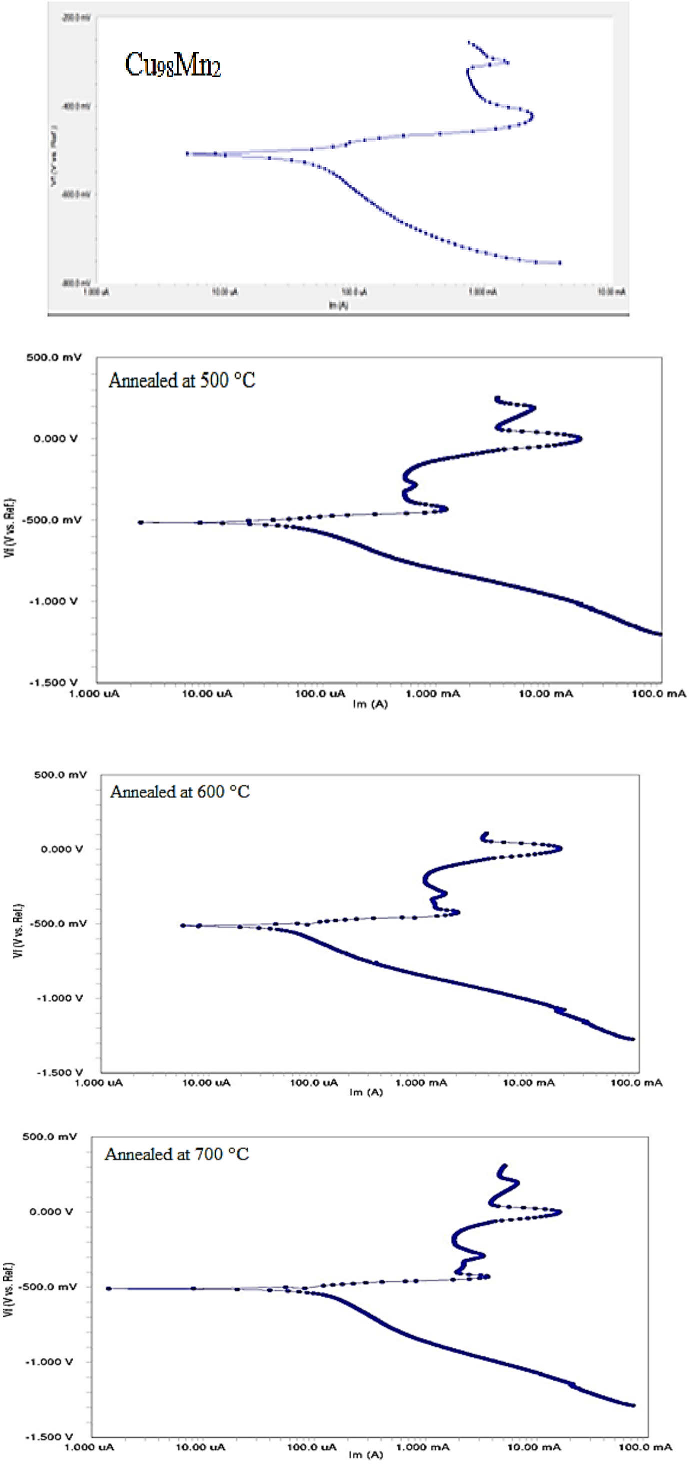

Figure 3. Electrochemical polarization curves of used alloys

Table 3. Corrosion potential (E_{Corr}), corrosion current (I_{Corr}), and corrosion rate (C. R) of used alloys

$Cu_{98}Mn_2$ alloy	I_{Corr} µA	E_{Corr} mV	C. R mpy
before	60	-509	30.47
500 °C	55.20	-512	30.29
600 °C	65.20	-516	32.18
700 °C	182.0	-511	89.64

EFM is a non-destructive corrosion measurement technique. The results of EFM experiments are a spectrum of current response as a function of frequency. The intermodulation spectrum of $Cu_{98}Mn_2$ alloy before and after annealed at 500 or 600 or 700 °C for two hours alloys in 0. 25 M HCl solutions are shown in Figure 4. The larger peaks were used to calculate the corrosion current density and the corrosion rate whish presented in Table 4. The corrosion current density and corrosion rate of $Cu_{98}Mn_2$ alloy in 025 M HCl increased after annealed at different temperature for 2 hours.

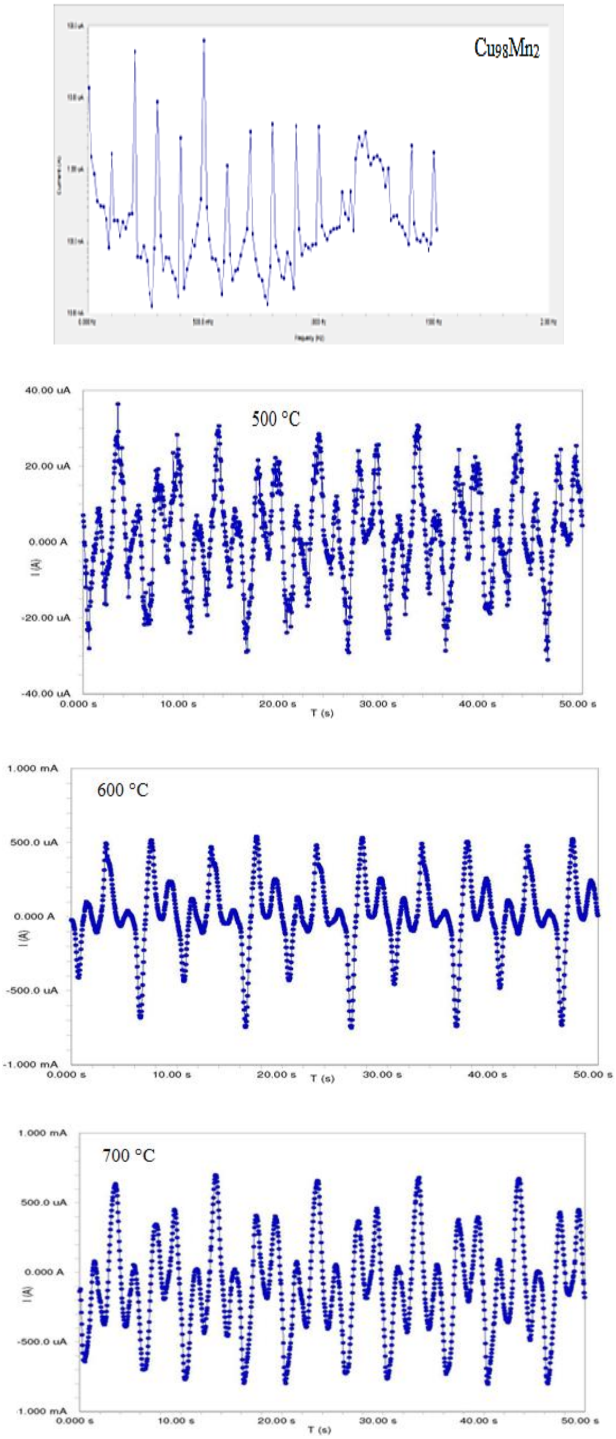

Figure 4. Intermodulation spectrum obtained by EFM technique for used alloys

Table 4. The corrosion current density (i_{corr}) and the corrosion rate (C. R) of used alloys

$Cu_{98}Mn_2$ alloy	i_{Corr} μA	C. R mpy
before	230.5	117.1
500 °C	254.9	139.7
600 °C	420.2	207.4
700 °C	802.8	928

IV. CONCLUSION

Significant changed in structure (formed phases such as intensity, broadness, area and position) $Cu_{98}Mn_2$ alloy after annealing at different temperature for two hours. Lattice microstrain of $Cu_{98}Mn_2$ alloy varied after annealed at different temperature for two hours. Vickers hardness of $Cu_{98}Mn_2$ alloy increased after annealed at 500 or 600 or 700 °C for two hours. Very little variation occurred in corrosion rate of $Cu_{98}Mn_2$ alloy after annealing at 500 or 600 °C for two hours. Significant increased occurred in corrosion current and corrosion rate of $Cu_{98}Mn_2$ alloy after annealing at 700 °C for two hours.

V. REFERENCES

[1] Lai M.O, Lu L, Lee W.L, J. Mater. Sci., 31:6 (1996) 1537-1543
[2] A. B. El-Bediwi, Radia. Eff. Def. Sol. 159 (2004) 539–542.
[3] M.J. Esfandyarpour, R. Mahmudi, Mater. Sci. Eng. A 530 (2011) 402–410
[4] A Chrysanthou, G Erbaccio, J. Mat. Sci., 30 (1995) 6339–6344
[5] Y. Z Zhan, G. D Zhang, Key Eng. Mat., 249 (2003) 227–232
[6] K. Ichikawa, M Achikita, Mat. Trans. JIM, 34 (1993) 718–724
[7] R. H Palma, A. O Sepulveda, Mat. Sci. Forum, 416-418 (2003) 162
[8] B Tiang, P Liu, K Song, Y Li, Ren F, Mat. Sci. Eng., A 435-436 (2006) 705
[9] D. B Rajković, A. Devečerski, J. Serb. Chem. Soc., 72 (2007) 45–53
[10] P. KJena, E.A.I GBrocchi, I.G. Solorzano, Motta M.S, Mat. Sci. Eng., A 371 (2004) 72–78
[11] J.H Ahn, I.H Song, Y.D Hahn, Mat. Trans. JIM, 37 (1996) 733–737
[12] A Mukhtar, D.L Zhang, C Kong, P Munroe, IOP Conference Series, Mat. Sci. Eng., 4 (2009) 012005
[13] B. D. Cullity and S. R. Stock, Elements and x-ray diffraction, 3rd edn, (Prentice Hall). 2001
[14] C. Suryanarayana, Prog. Mater. Sci. 46: 1 (2001)